Molecular Crystals and Liquid Crystals
Publication details, including instructions for authors and subscription information:
http://www.tandfonline.com/loi/gmcl16

Microemulsions and Liquid Crystals

D. Langevin [a]
[a] Laboratoire de Spectroscopie Hertzienne de l'E.N.S., 24, rue Lhomond, 75231, Paris, Cedex 05, France
Version of record first published: 17 Oct 2011.

To cite this article: D. Langevin (1986): Microemulsions and Liquid Crystals, Molecular Crystals and Liquid Crystals, 138:1, 259-305

To link to this article: http://dx.doi.org/10.1080/00268948608071764

Mol. Cryst. Liq. Cryst., 1986, Vol. 138, pp. 259–305
0026-8941/86/1384–0259/$25.00/0

Printed in the United States of America

Microemulsions and Liquid Crystals

D. LANGEVIN

Laboratoire de Spectroscopie Hertzienne de l'E.N.S. 24, rue Lhomond—75231 Paris Cedex 05—France

(*Received April 25, 1985*)

I. INTRODUCTION

A. Definition

Microemulsions are dispersions of two unmiscible liquids made with surfactant molecules.[1] Most of the time one of these liquids is water although non aqueous microemulsions can be made with polar liquids.[2] Water can eventually contain dissolved salts. The other liquid is of apolar character and is generally called "oil," even when dealing with organic solvents like benzene.

Like emulsions, microemulsions often contain oil or water droplets, surrounded by a surfactant layer, and dispersed into a water or an oil continuous phase (Figure 1). By analogy with emulsions, they are called oil in water (O/W) or water in oil (W/O) microemulsions. The droplet size is however much smaller in microemulsions: about 100 Å, whereas it is about 1 μ in emulsions. For this reason microemulsions are reasonably optically transparent. In the following we will see that they are thermodynamically stable systems, again because of this very small characteristic dispersion scale. We will also see that other microstructures can be observed, analogous to distorted smectic phases.

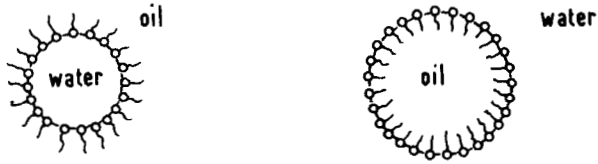

FIGURE 1 Droplets structure in W/O or in O/W microemulsions.

Oil-water-surfactant mixtures show very complex phase equilibria. Liquid crystalline phases are frequent,[3] and it is not always obvious to distinguish them from microemulsion phases. Lyotropic lamellar phases with small optical birefringence and small viscosity are commonly observed close to microemulsions domains in the phase diagram[4] (Figure 2). However, liquid crystalline and microemulsion regions seem always disconnected. A more serious difficulty appears when molecular mixtures of oil, water and surfactant, have to be distinguished from mixtures where well defined interfaces between oil and water exist on a microscopic scale. Apparently, these two kinds of mixtures continuously transform one into the other without any sharp transition in the phase diagram. For this reason, several authors proposed to extend the name microemulsion to molecular mixtures. From our part we will restrict the term microemulsion to the systems presenting a well defined microstructure.

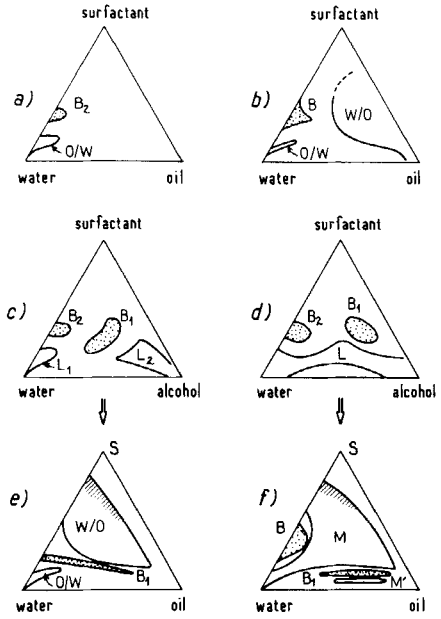

FIGURE 2 Typical oil-water-surfactant ternary phase diagrams; a) ionic surfactant; b) amphoteric or non ionic. Typical water-alcohol-surfactant ternary phase diagrams; c) long chain alcohol; d) short chain alcohol, and their evolution when oil is added: pseudo ternary diagrams at fixed surfactant/alcohol ratio; e) long chain alcohol; f) short chain alcohol. B are birefringent domains, B_1 lamellar and B_2 hexagonal liquid crystalline phases. M, M' are microemulsions domains. Other liquid crystalline or gel phases may be present, but do not have been represented.

Finally, there is also a continuity between microemulsion regions in the phase diagram and the micellar systems obtained with water-surfactant mixtures or oil-surfactant mixtures (reverse micelles). Several authors pointed out that there is a difference between microemulsions containing small and large amounts of oil (or water). In the first case, the microemulsions are dispersions of swollen micelles in water (or oil). The oil (or water) molecules are very close to the interfacial surfactant layer and behave very differently than bulk oil (or water). When the oil (or water) amount in the dispersion increases, the oil (or water) properties progressively tend toward their bulk properties. Several methods were proposed to locate roughly this limit in the phase diagram and the name "microemulsion" is sometimes restricted to the systems where both oil and water have "bulk" properties.[6]

In this paper, we will use the following definition for microemulsions: oil-water-surfactant mixtures, optically transparent and thermodynamically stable (excluding emulsions), optically isotropic and of small viscosity (excluding liquid crystals), where well defined interfaces between oil and water exist at a microscopic scale (excluding molecular mixtures). The last point is obviously the most difficult to check and is the source of many existing controversies in the literature. This point will be discussed in more detail later on. Finally, excepted in very few cases, we will not make a difference between microemulsions and swollen micellar systems.

B. Historical background

Microemulsions have many practical applications in detergency, oil recovery, improvement of chemical reactivity including photochemistry and solar energy conversion, drugs delivery, . . . They have been used well before their specific properties were recognized. One example is the formulation found by Australian housewives the last century to wash the wool: they mixed soap flakes (surfactant) with white spirit (cosurfactant), eucalyptus oil and water. The result was a transparent fluid with which rinsing was not necessary and where the oil acts as a softener. This example illustrates the important fact that a cosurfactant is frequently needed to formulate microemulsions. Here the cosurfactant is an alcohol, but it can also be an amine, an acid, a short chain polyethylene glycol. . . . We will see in the following that the role of the cosurfactant is extremely complex, and is the source of many difficulties in modelling theoretically microemulsions.

The first microemulsion of the commerce was probably made by G. Rodawald in the U.S.A. in 1928.[1] It was a dispersion of Carnauba wax in water, made with oleic acid, potassium hydroxide and borax. The first two additives react to give potassium oleate which is the surfactant. Borax allows to keep some free oleic which is the cosurfactant.

The Carnauba wax emulsions became the basis of self polishing floor wax formulas. Upon application, the water evaporates and the oil droplets coalesce to form a uniform layer. The product thus requires no buffing to make it shine. Nowadays polymer (latex) emulsions have replaced the wax emulsions for floor polishing applications. They are also widely used in the paint industry. Their drying process is basically the same as for wax emulsions.

The concept of stability of Carnauba wax emulsions found rapidly imitators in other fields like cutting oils. The first cutting oils were mineral oil emulsions: the oil is a lubricant, the water, a coolant, and the surfactant is both an emulsion stabilizer and a corrosion inhibitor. The emulsion is usually recirculated and after a few cycles, it loses progressively stability and efficiency. Microemulsions can be made with mineral oil and used as cutting oils. They are stable in the recirculation process. These systems were commonly used as early as 1930.

Microemulsions also became largely used in detergent formulations. The incorporation of oil in aqueous soap solutions has many advantages: oil solubilization and removal after suspension in the water are improved, redeposition on the clothes is prevented. The first commercial formulations in the late 1920's were pine oil microemulsions and were the precursors of modern anti-redeposition products.[1] Microemulsions also allow to achieve the combination of the detergent properties of aqueous soap solutions and of dry cleaning methods, by incorporating organic solvents in the soap solutions. The O/W microemulsions obtained in this way have much better efficiencies than the pure solvents. They allow to reduce considerably not only the amount of these solvents but also their vapour pressures. This is very important in practice because of the solvent's toxicity.

The fundamental research on microemulsions was initiated by J. Schulman and coworkers around 1940.[7] Extensive investigations using low angle X-ray scattering, ultracentrifuge, electron microscopy, NMR, etc., led them to consider that these systems were a new kind of colloidal dispersion. They identified the presence of very small droplets of either oil in water (O/W microemulsion) or water in oil (W/O microemulsion). These structures were small scale version of

the emulsions ones, and the new dispersions were named microemulsions for the first time in 1958.[8]

Schulman and coworkers also tried to explain the thermodynamic stability of microemulsions and the spontaneous emulsification of oil and water. They proposed that the surfactant reduced the initial oil-water interfacial tension, typically of about 50 dyn/cm, down to very small and even negative values. In this way the free energy of the dispersed system could be lower than the initial one although the oil-water interfacial area had considerably increased.

It was shown later on by E. Ruckenstein and coworkers[9] that negative surface tensions were not necessary to form microemulsions. They introduced the concept of dispersion entropy in the free energy and were able to show that small but positive tensions, about 10^{-2} dyn/cm, gave reasonable values for the size of the droplets. This size is noticeably smaller than in emulsions: typically 100 Å instead of 1 μ. They demonstrated in this way that microemulsions were thermodynamically stable systems.

Another important aspect of microemulsion properties is their interfacial behaviour. They can be in equilibrium with excess oil or excess water or both excess oil and water. The corresponding interfacial tensions are also ultralow, below 10^{-2} dyn/cm. The concept of ultralow tensions found an interesting application in enhanced oil recovery.[10]

The recovery of oil from a reservoir is basically done in three stages. In a primary process, oil is forced out through production wells due to the pressure of natural gases. When the production is stopped, water is injected to force further oil out. After this secondary process, the oil recovery is about 30–50% of the oil in place. To recover the remaining oil, tertiary or enhanced recovery processes have to be used. The remaining oil is trapped in the pores of the reservoir rocks by capillary forces. Microemulsions allow to decrease the interfacial tension between oil and water by several orders of magnitude and thus improve the oil recovery, theoretically up to 100%.

The first processes using surfactants were patented around 1960. They did not use yet microemulsions, and the low tensions, below 10^{-2} dyn/cm, were obtained with small amounts of surfactant. The recovery efficiency was greatly reduced by surfactant adsorption on the rocks surface. Later on, patents using the microemulsions which could be in equilibrium with both excess oil and water were proposed. In the following we will see that the origin of the low tensions is not different than in the systems with small surfactant concentrations,

but the microemulsions act as a surfactant reservoir. Let us mention that although low tensions are a necessary requirement, other microemulsion properties can favour recovery enhancements: improval of rock wetting, small interfacial viscosities encouraging the oil ganglia to coalesce and to form an oil bank, partial solubilization of heavy oils, which could be effective even in tar sand extraction. . . . It can be pointed out at this stage that sometimes a problem in tertiary recovery with microemulsions is to avoid the formation of liquid crystalline phases very frequent in the oil-water-surfactant mixtures. Indeed when these phases have large viscosities they can stop the reservoir.

The applications of microemulsions in oil recovery greatly stimulated the development of the research in the field. It became rapidly clear that the "optimal" microemulsions which could coexist with both oil and water in a three phase equilibrium were not dispersions of droplets either of the W/O or O/W types. In 1976, S. Friberg[11] and L. Scriven[12] proposed that they could be bicontinuous i.e. both water and oil continuous. Friberg's picture looks like a distorted lamellar phase, whereas Scriven's one was a cubic liquid crystalline phase (Figure 3). The exact nature of the structure has not yet been satisfactorily elucidated. Another unsolved question is the inversion mechanism between W/O and O/W structures that occurs continuously in some systems (Figure 2f). The intermediate formation of bicontinuous structures has been postulated, but not yet proved satisfactorily. These questions stimulated a number of theoretical and experimental works, and the field of research is today extremely active.

The dynamic and in particular the transport properties of microemulsions are still much less well understood than their structural

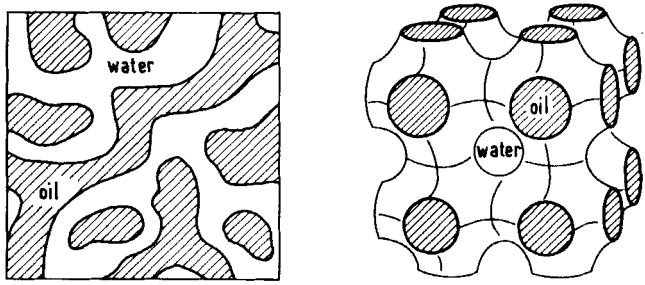

FIGURE 3 Two extreme pictures of a bicontinuous structure: a completely random one and a regular one having a cubic symmetry.

properties. For instance, the viscosity of the liquid crystalline like bicontinuous media proposed by Scriven and Friberg should be very high. Experiments indicate on the contrary that microemulsions are small viscosity fluids. The answer to the paradox lies probably on the fact that microemulsions structures are transient. Their lifetime is governed by exchanges of molecular constituents between different structural elements. The characteristic times involved are of the order of 10^{-6}–10^{-7} sec.[13] Entities solubilized in the water or oil microdomains can be exchanged between these domains almost as fast as in molecular solutions. This property is of a fundamental importance in many practical applications like for instance chemical reactivity: microemulsions are extraordinary efficient catalysts, because of the very large contact area between oil and waters domains. Reactants solubilized in the different domains could only react when ever exchanges take place.

Microemulsions potential applications in chemistry are numerous. They improve by orders of magnitude the yield of reactions involving two unmiscible liquids, like for instance esterification of polyalcohols (polyglycerol and others) with fatty acids. Beside the enormous increase in contact area between the constituents, the interfacial surfactant layer probably allows to fix the substrates in specific configurations and orientations. The micro-environment may resemble to active sites of enzymes. This would explain the specific enhancement of many reactions, much larger than what could be expected on the basis of simple partitioning of reactants in oil and in water. Microemulsions are good specific catalysers. They can make possible new reactions: ionic polymerisation in apolar solvents, organic electrosynthesis[14] . . .

Microemulsions can also be used to prepare very small solid particles like metallic catalysts, magnetic colloids, microlatices, . . . Particle sizes are less than or of the order of 100 Å and are very uniform. The preparation involves a chemical reaction in the dispersed medium: metallic ions reduction, in situ polymerisation (which can be initiated with light owing to the transparency of the medium, contrary to the classical emulsion polymerization methods).[15] In this way, platinum particles of 60 Å diameter, monodispersed within 10% have been prepared.[16] The growth mechanisms of these particles during their preparation (their final diameter is generally larger than the microemulsion droplets ones) is actively studied but still very poorly understood.

The exchanges of constituents in microemulsions can be sufficiently slow in well chosen systems to allow to separate charges during long enough periods in photochemistry devices for solar energy conver-

sion.[17] This new requirement is very different from the reactivity enhancements discussed above, where fast constituent exchanges were required. In the following we will indicate how these multiple aspects can be obtained in practice. They are a good example of the microemulsions flexibility for practical applications.

We will finally mention some potential applications of microemulsions in biotechnology. One of the most interesting is certainly the "artificial" blood. It has been known for long that the fluorocarbons compounds solubilize oxygen, like homoglobin. But they are water insoluble. Microemulsions can be made with these compounds by using appropriated surfactants. These systems are stable and can serve as intravascular oxygen and carbon dioxide transport agents. Their main disadvantages are their relative toxicity due to the elevated surfactant content. They will probably begin to be used as partial blood substitutes like the fluorinated emulsions (about 50% in volume) were in Japanese hospitals since 1979.

Microemulsions are also investigated for drugs delivery. It has been proposed to use them to administrate drugs which are soluble in oil.[1] For water soluble drugs they are difficult to use directly because of oil toxicity. The difficulty can be avoided by using a polymerizable surfactant. After microemulsion formation and polymerization of the interfacial film, the oil can be replaced by an appropriated aqueous phase.[18] The advantage of microemulsions over vesicles currently investigated in this field of research is the very small size of the carrier elements; contrary to vesicles they are unlikely to interact with the cell constituents.

This short presentation of microemulsions properties and applications explains why they are a very active subject for both fundamental and applied research. In the following we will present in more details the state of theoretical knowledge about these systems: phase diagrams, thermodynamic stability, structure, phase separation mechanisms, low interfacial tensions, and dynamic properties.

II. PHASE DIAGRAMS

A. Microemulsions composition

Microemulsions are usually quaternary mixtures of oil, water, surfactant and cosurfactant. Model systems have been often studied in relation with oil recovery; oils are linear alkanes in the range heptane to hexadecane, cyclic or aromatic hydrocarbons like cyclohexane,

benzene or toluene. Water can contain sodium chloride as model salt. Salt is not considered as a new component of the mixtures because in many cases, the water salinity is roughly the same in the coexisting phases obtained from a given mixture.[19]

Surfactants are petroleum sulfonates. Several common constituents of the commercial mixtures are listed in Figure 4. These long chain surfactants are very difficult to purify. For this reason purer shorter homologs like sodium octyl benzene sulfonate (OBS) have frequently been used in model systems. A commercially available pure surfactant, the sodium dodecyl sulfate (SDS), has also been extensively studied. A large number of data on the micellar and liquid crystalline phases was already available for the simpler water-SDS mixtures and this was a great advantage in understanding the more complex microemulsion mixtures. Data on the water-SdS (sodium decyl sulfate)—alcohol micellar and liquid crystalline phases also exist.[20]

All the above surfactants are of the "anionic" type. "Cationic" surfactants like dodecyl ammonium and hexadecyl ammonium chlorides or bromides have also been extensively studied although they are useless for oil recovery purposes, since they adsorb too strongly on the reservoir rocks. However they are very interesting model surfactants because homolog series of pure compounds can be synthetized easily. Nonionic surfactants like the polyoxyethylene glycols (C_n E_m) are also currently used to formulate microemulsions. These microemulsions are relatively insensitive to salt addition contrary to

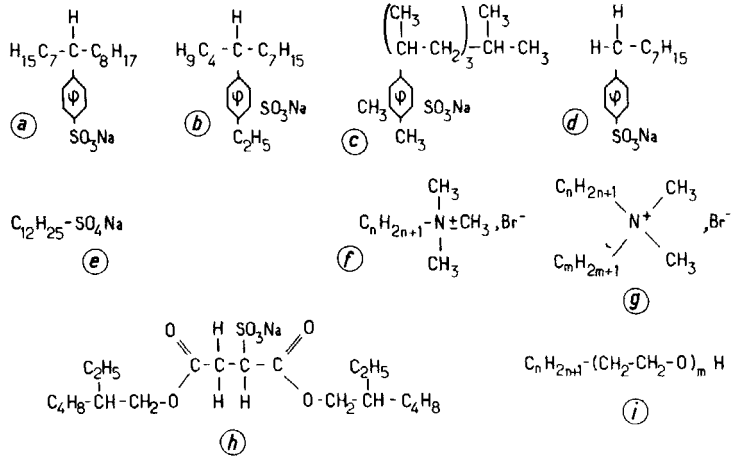

FIGURE 4 Examples of surfactants commonly used to formulate microemulsions: *a* to *c* are petroleum sulfonates, *d* is OBS, *e* is SDS, *f* and *g* are cationic surfactants, *h* is AOT, and *i* a non ionic surfactant.

ionic surfactant microemulsions, but they are much more temperature sensitive. Some of these surfactants can be used without cosurfactant. Let us recall that the shorter homologs of the series have to be considered as cosurfactants rather than surfactants. Among the other surfactants that can be used without cosurfactant let us mention the extensively used sodium salt of diethylhexyl sulfosuccinate (AOT) and several double chain cationic surfactants like the didodecyl dimethyl ammonium bromide.

Cosurfactants are necessary when the surfactant is too soluble in oil or in water, like formost ionic surfactants. Alcohol cosurfactants are frequently used. The choice of the alcohol depends on the oil and on the surfactant and as we will see later on the type of microemulsion that has to be made. Frequently the alcohols are in the range—propanol to heptanol. Like surfactants, they have to be located at the interface between oil and water to play the role of a cosurfactant. For this reason their solubility in oil and water has to be as small as possible. Unfortunately these solubilities are always much larger than the surfactant ones. This is the source of many difficulties in modelling such microemulsions, since the partitioning of the alcohol between oil, water and interfacial regions is not easy to determine.

B. Winsor phase diagrams

Winsor proposed a very simple representation of oil-water-surfactant phase diagrams (Figure 5).[21] He used the triangular representation for ternary mixtures. Let us recall briefly the way in which such diagrams can be read (Figure 6):

—for a point M_1 in a single-phase region, the amount of a given constituent A is proportional to the distance M_1A between the point M_1 and the triangle apex corresponding to the constituent A;

—for a point M_2 in the two-phase region, the two phases compositions correspond to the points P and Q where the "tie line" where

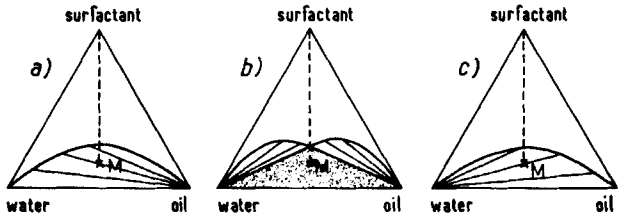

FIGURE 5 Winsor phase diagrams.

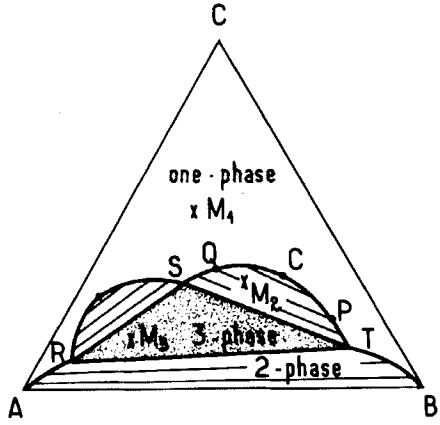

FIGURE 6 Three component phase diagram showing multiphase equilibria.

M_2 is located cuts the phase boundary. The relative amounts of the two phases are proportional to the distances M_2P and M_2Q;

—for a point M_3 in the three-phase region, the three phases compositions are those of the three-phase triangle RST apexes; the relative amounts of the three phases are proportional to M_3R, M_3S and M_3T.

In the Winsor representation, oil and water are considered to be unmiscible and one side of the three phase triangle is the oil-water axis. The mixture surfactant-cosurfactant is treated as a single component $s + c$. Liquid crystalline phases are not taken into consideration. The tie lines in the two phase regions have a common point: the water or oil apex. A single phase microemulsion is encountered in the surfactant rich part of the phase diagram.

For a given mixture containing equal amounts of oil and water and a small surfactant concentration, represented by the point M in Figure 5, different types of phase equilibria can be obtained:

a. a microemulsion in equilibrium with excess oil: Winsor I equilibrium

b. a microemulsion in equilibrium with both excess oil and water: Winsor III equilibrium

c. a microemulsion in equilibrium with excess water: Winsor II equilibrium.

The evolution of type a diagrams towards type c diagrams reflects the evolution of the surfactant solubility on water and in oil: type a

diagrams corresponds to a water soluble surfactant and type *c* diagrams to an oil soluble surfactant. This evolution can be obtained in different ways in practice; for ionic surfactants, the addition of salt or of an alcohol lower their hydrophylicity. For non ionic surfactants an increase in temperature plays the same role.

Real phase diagrams are of course more complicated.[22,23] First, they often exhibit liquid crystalline phases in the surfactant rich region.[12] Second, the mixtures surfactant + cosurfactant cannot be treated as a single component. The real phase diagram which is a tetrahedron can be represented by different triangular cuts for instance at a fixed surfactant/cosurfactant ratio (Figure 7). The tie lines and the 3-phase triangles for a given point in one triangular cut generally belong to other triangular cuts and the phase diagrams are considerably distorted (Figure 7).

The truly ternary systems with a single pure surfactant like aerosol *OT*, and non ionic surfactants are closer to the Winsor description.[24,25] However, the three phase triangle does not touch the water-oil axis as in the schematic Winsor diagrams. The tie lines of the two-phase region do not pass through the oil and the water corners. As a consequence critical plait points *C* are observed in these phase diagrams (Figure 8). Sometimes these critical points can be close to the three phase triangle, one side of which becomes very short. In the limit case where the critical point touches the three phase triangle, the three phase region disappears and is replaced by a two-phase region. This critical point is called critical end point. This situation can also be found in a four-component phase diagram where the three-phase region is formed of stacked triangles.[26] The locus of the apexes of these triangles is a curve which can be continuous (Figure 9). In this case two critical end points are found in the tetrahedron C_1 and C_2. In ternary mixtures, the two critical end points can be reached for instance by varying the temperature which plays the role of a fourth component.

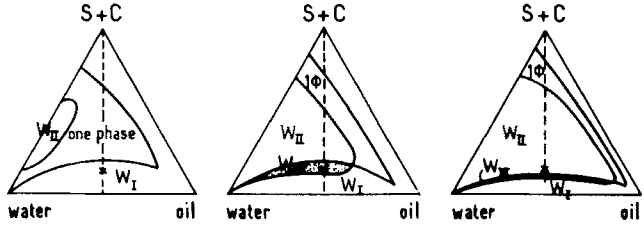

FIGURE 7 Typical pseudo three-component phase diagrams for fixed ionic surfactant (*S*)—cosurfactant (*C*) ratio. Evolution with increasing water salinity.

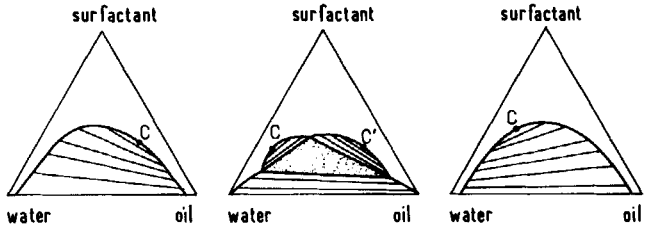

FIGURE 8 Real three-components phase diagrams, to be compared with the ideal Winsor diagrams of Figure 4.

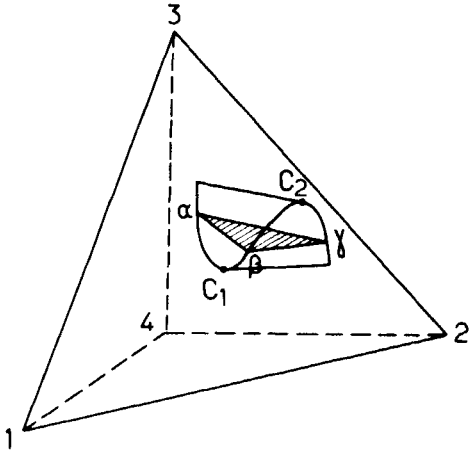

FIGURE 9 Quaternary phase diagram showing a three phase domain, one of the three phase triangles α β γ, and the two critical end points c_1 and c_2.

The distance of the three phase triangle to the oil-water axis decreases with increasing surfactant chain length, thus ressembling progressively to the ideal Winsor diagrams.

C. Other types of phase equilibria

Winsor type diagrams describe microemulsions in equilibrium with excess oil and/or water. The slightly modified diagrams of Figure 8 describe microemulsions in equilibrium with other microemulsions, and the occurrence of critical plait points and critical end points. Microemulsions can also be in equilibrium with liquid crystalline phases. The corresponding details in the phase diagram are usually very complex. We will only present here an example which has been studied

in detail in the literature and is associated to large periodicity smectic phases.

These phases were evidenced in anionic surfactant systems containing no salt.[27,28] They are connected to the liquid crystalline phases of the simpler water-surfactant-alcohol mixtures. Let us consider the evolution of the phase diagrams when alcohol is added. The ternary mixtures oil-water-surfactant show the existence of swollen aqueous micelles L_1 and swollen hexagonal phases B_2 (Figure 2a). When a long chain alcohol is added the size of the L_1 region, increases. Moreover, a swollen reverse W/O system, connected to the reverse micelles region L_2 in the water-surfactant-alcohol diagram (Figure 2c and e), develops. Similarly a lamellar liquid crystalline region B_1 connected to the corresponding B_1 region in the water-surfactant-alcohol diagram is also present. In this type of diagram the O/W and the W/O microemulsions regions are separated by the liquid crystalline region B_1 and the inversion of structure is discontinuous.

When a shorter chain alcohol is used, the micellar region in the ternary water-surfactant-alcohol diagram is much more extended, and the normal micelles L_1 and reverse micelles L_2 domains are connected (Figure 2d). In the quaternary diagram the O/W and the W/O microemulsions regions are also connected and the inversion is continuous. The liquid crystalline region B_1 splits into two parts in several triangular cuts of the phase diagram. The microemulsion region is also split in the same cuts although one of the pieces is extremely small: region M', Figure 2f. This small region is connected to the whole single phase microemulsion region, close to the water apex in the water-oil-surfactant face of the tetrahedron. Although the microemulsions M' are oil rich systems their electrical conductivities are very high indicating that they are water external systems.[28] They exhibit large streaming birefringence showing that they contain probably elongated swollen micelles.[27] Similar properties have been reported for several truly ternary systems with double chain cationic surfactants.[29]

A smaller region M'' close to M' where microemulsions also exhibit streaming birefringence is associated to very complex phase equilibria including up to four phases: two ordinary microemulsions, a microemulsion showing streaming birefringence and a liquid crystalline phase.[27] The four-phase region is extremely small and is the locus of the end of a line of critical plait points which are usually found in the oil rich part of these short chain alcohol type of diagrams.[27] The complicated features of these phase diagrams are not completely understood.

In particular the four-phase equilibrium, the properties of flow birefringent microemulsions still deserve more work.

The simpler equilibria microemulsion-liquid crystalline phase are also under study as well as the liquid crystalline phase properties. These phases were identified to be smectic phases of large periodicities, up to 150 Å.[4] They contain a large number of curved defects which probably prefigurates the microemulsion droplets.[30] The critical plait points in this oil rich region are also close to the liquid crystalline domain. They have been extensively studied in the literature. The results will be described later on in Chapter VII. The connection between the critical behavior and the presence of liquid crystalline phases is however far from being understood.

More generally, the existence of microemulsions in an oil-water-surfactant phase diagram is accompanied by the existence of liquid crystalline phases. For instance liquid crystalline phases are not encountered in the oil-water-non ionic C_n E_m diagrams with the shorter homologs of the serie which should be considered as cosurfactants.[25] The formation of liquid crystalline phases with the higher homologs probably reflects the ability of the system to form interfaces at a microscopic scale between oil and water regions. In the next paragraph, we will see that the local rigidity of these interfaces probably determines whether a microemulsion (small rigidity) or a liquid crystal (high rigidity) is formed.

III. THERMODYNAMIC STABILITY

A. Structural models

The starting point of the statistical thermodynamics calculations for microemulsions is to work out a satisfactory structural description of the medium. The earlier treatments were based on the droplet structure proposed by Schulman. It became however necessary to include the bicontinuous structures proposed by Friberg and Scriven.

A very elegant description was then proposed by Y. Talmon and S. Prager, with a random interspersion of Voronoi polyhedra filled with either oil or water; the surfactant lies at the interface between oil and water domains and is supposed to have a negligible volume[33] (Figure 10). If the water volume fraction ϕ_w is less than a certain value ϕ_p, the oil phase is continuous and the water polygons are isolated or form finite size groups; they are surrounded by the oil.

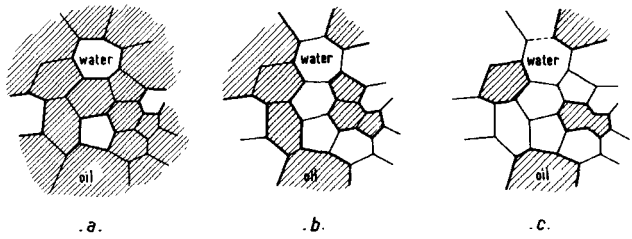

FIGURE 10 Voronoï tesselation for increasing water to oil ratio.

These water polygons represent the microemulsion droplets and the whole picture, a water in oil microemulsion. ϕ_p in the model is equal to 0.185. For higher water volume fractions, part of the water become sample-spanning, i.e., there exists a continuous path of water reaching from one side of the sample to the other. The transition at ϕ_p is typical of a "percolation" phenomena. A second transition of the same type exists for $\phi_w = 1 - \phi_p$: the oil polygons are no longer connected on a large scale and the microemulsion turns to the O/W type. The medium is bicontinuous between ϕ_p and $1 - \phi_p$.

Later on, P. G. de Gennes[34] proposed to identify the characteristic size of the polyhedra as the persistence length of the interfaces ξ_k: consecutive interfacial regions with an area ξ_k have independent orientations and the interface is essentially flat at scales smaller than ξ_k. He also proposed to simplify the Talmon-Prager description by dividing the whole space into adjacent cubes each of linear size ξ_k randomly filled by either oil or water. The essential features of the original model are conserved in this way, and the calculations, considerably simplified.

B. Statistical thermodynamical treatment

The thermodynamic stability can now be discussed with the Ruckenstein ideas generalized to the Talmon-Prager-De Gennes model, which describes O/W W/O and bicontinuous microemulsions as well. If N is the total number of cubes, and γ the oil water interfacial tension, the interfacial free energy of the medium is:

$$F_i = 6\,\gamma\,N\,\phi_w\,(1 - \phi_w)\,\xi_k^2 \tag{1}$$

the entropy of dispersion is:

$$S_d = -k\,N[\phi_w \ln \phi_w + (1 - \phi_w)\ln\,(1 - \phi_w)] \tag{2}$$

The total free energy $F = F_i - TS_d$ is formally identical to that of a lattice gas problem. The result is well known: when the coupling energy between adjacent sites $\gamma\xi_k^2$ is weaker than kT, or more precisely when:

$$\gamma < \gamma_c \sim 0.3\, kT/\xi_k^2$$

a stable single phase microemulsion can be formed. γ and ϕ_w being given, the optimum value of ξ_k, is obtained by minimizing F.

The requirement $\gamma < \gamma_c$ implies that positive but very small interfacial tensions have to be reached. The oil-water interfacial tension γ_0 in the absence of surfactant is of the order of a molecular energy kT divided by the square of a molecular distance a^2 ($a \sim 1$ Å). If the scale of the oil-water dispersion ξ_k is about 100 Å, then γ has to be reduced by four orders of magnitude. Typically $\gamma_0 \sim 50$ dyn/cm thus leading to $\gamma \lesssim 10^{-2}$ dyn/cm. Emulsions are formed typically when $\gamma \sim 1$ dyn/cm, value easily obtained with usual surfactants. It is less easy to reach smaller values unless a cosurfactant is used. This explains why microemulsions are less frequently encountered than emulsions. We will discuss the problem of low tensions in more details later on (§ IV).

The phase equilibria generated by the above statistical model is very simple: a single phase domain for $\gamma < \gamma_c$, i.e. in the surfactant rich region and a two-phase domain for $\gamma > \gamma_c$, in the surfactant poor region. A critical point is obtained for $\phi_w = 1/2$. Oil and water play entirely symmetrical roles in the phase diagram.

We have seen that real phase diagrams are more complicated and in particular that three phase equilibria exist. It is possible to generate such equilibria by introducing a curvature term in the free energy.

C. Curvature energy

Curvature effects contributions F_c in the free energy are very small compared to interfacial free energies F_i in many physical situations. Microemulsions are an exception, because F_i is unusually small.

1. *Geometrical considerations*

Baucroft proposed in 1927[35] a rule for the determination of the continuous phase in emulsions: the trend is to have the best solvent of the surfactant outside the droplet.

More quantitative predictions have been made recently by Ninham and Mitchell for ionic surfactants on the basis of packing consider-

ations and on the analysis of the stresses on the two sides of the surfactant layer.[36] If v is the alkyl chain volume, Σ the area per polar head and l_c the alkyl chain length, they obtained a very simple result: when $v/\Sigma l_c$ is less than one, oil swollen aggregates will be formed and when $v/\Sigma l_c$ is larger than one, reverse system, i.e. water swollen aggregates will form. If $v/\Sigma l_c$ is close to one, the mean curvature is about zero and bicontinuous like microemulsions will be formed (Figure 11). In this theory unfortunately the role of the cosurfactant and of an eventual oil penetration in the surfactant layers is not explicitly accounted for.

Similar considerations were made by Robbins[37] for non ionic surfactants and by Cantor for copolymers surfactants.[38]

These theories show the existence of an optimum radius of curvature R_0 and lead to expressions for the curvature free energy per unit area close to:

$$F_c = K\left(\frac{1}{R} - \frac{1}{R_0}\right)^2 + F_{co} \tag{3}$$

where K is a curvature modulus, R the actual radius of curvature and F_{co} a constant term. For $1/R_0 = 0$ Eq. (3) reduces to the splay energy of a single layer of a smectic liquid crystal.

That the free energy F_c would consist of terms proportional to the first and second powers of the mean curvature besides a constant term is as was concluded by De Gennes and Taupin[34] from Helfrich's earlier phenomenological analysis of the elastic properties of lipid bilayers,[39] and as pointed out independently by S. Safran.[40]

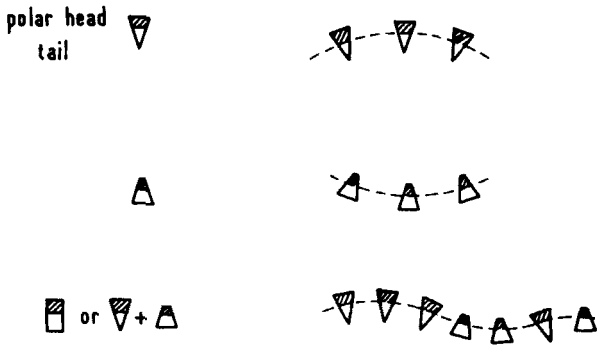

FIGURE 11 Relation between surfactant molecular shape and spontaneous curvature. Possible segregation effects.

2. *Consequences for the phase diagrams*

When oil in water droplets are favoured for example, the Winsor I type of equilibrium can be easily understood in a phenomenological way:[40] for small oil concentrations, droplets of radius R less than R_0 are formed. As oil is added, the droplets grow in radius. When R reaches R_0, the bending energy (3) is minimized by constraining all droplets to have this minimum size and expelling the excess oil into a separate phase. Winsor II equilibria can be explained in a similar way.

Three-phase equilibria were found slightly artificially in the original model by Talmon and Prager. They assumed that interfaces of finite curvature $\pm 1/R_0$ were equally favoured with respect to the flat interface. They obtained three-phase equilibria between three microemulsion phases of curvature O, $\pm 1/R_0$.

Real Winsor III equilibria correspond rather to a microemulsion of zero average curvature with excess oil and water. By further modifying the Talmon-Prager-De Gennes model, and by imposing a microscopic cell-size cut off, B. Widom was able to demonstrate theoretically the existence of these Winsor III equilibria.[41]

The appearance of liquid crystalline phases are probably strongly related to curvature energies. De Gennes and Taupin have shown that if θ is the angle between the two normals, defining the local orientation of the interfaces, at two points O and r, one has:[34]

$$\langle \cos\theta \rangle = \left(\frac{a}{r}\right)^{kT/2\pi K} \tag{4}$$

law which shows some classical features of two-dimensional fluctuations and which also hold for two dimensional nematics.[42] Equation 4 allows to define the persistence length ξ_K in the following way: at distances r smaller than ξ_K the angle θ is small on the average while at distances r larger than ξ_K it is large. Choosing for instance $\langle \cos\theta \rangle = 1/e$ as the cross-over value,[34] one obtains from Eq. (4):

$$\xi_K = a \exp[2\pi K/kT] \tag{5}$$

Thus the persistence length is extremely sensitive to the value of the curvature modulus K. If for instance K has a value comparable to that of thermotropic liquid crystals $K \sim 10^{-13}$ erg, then $2\pi K/kT \sim 15$ and ξ_K is about one million times larger than a molecular length: the interface is stiff, and the structure is ordered leading to a liquid

crystalline phase. If K can be decreased by a factor of 5, for instance by adding a short chain alcohol which is known to desorganise the interfaces (Figure 12), then $\xi_K \sim 20\ a \sim 200$ Å and the interface, observed at scales larger r than 200 Å is strongly wrinkled. In practice the liquid crystalline phases contain indeed less alcohol than the nearby microemulsion phases (Figure 2f).

Safran et coworkers[43] also predicted transitions between microemulsions and lamellar liquid crystalline phases but at fixed K, i.e. for instance in a single surfactant ternary system, and by varying R/R_0. They even found the possible existence of microemulsions containing elongated aggregates. This picture can be appropriate to describe the region M' in the phase diagram of Figure 2f. The transitions between spherical, cylindrical and lamellar phases are first-order. They further considered the general Helfrich picture in which the curvature energy also contain a "saddle" term with a corresponding elastic constant $\bar{K}$:

$$F_c = \frac{K}{2}\left(\frac{1}{R_1} + \frac{1}{R_2} - \frac{2}{R_0}\right)^2 + \frac{\bar{K}}{2}\left(\frac{1}{R_1} - \frac{1}{R_2}\right)$$

where R_1 and R_2 are the two local radii of curvature of the interface. The saddle splay energy which favours $R_1 = R_2$ (i.e. spheres or lamellar) reduces the range of stability of the cylindrical phase and for $\bar{K}/K > 1/3$ eliminates it altogether.

Up to now we have not introduced the interactions between the aggregates. We were therefore unable to describe the phase equilibria close to the critical points where two almost identical microemulsion phases coexist. This point will be treated in the next paragraph.

3. Role of the cosurfactant

We can summarize here the role of the cosurfactant:

—First, it allow to reduce the oil-water interfacial tensions to much lower values than the surfactant alone.

—Second, it contributes to fix the spontaneous curvature of the interfacial layers. It can also migrate towards the regions of strong (or normal) curvature. This is qualitatively indicated in Figure 11.

FIGURE 12 Disordered mixed surfactant layer and organized single surfactant layer.

Let us recall that short chain alcohols allow to invert continuously W/O towards O/W structures. This has never been reported in ternary mixtures with a single pure surfactant where the spontaneous curvature can not be varied.

—Third, it contributes to lower the elastic moduli by desorganizing to some extent the interfacial layers (Figure 13). As we have seen, this favour microemulsions against liquid crystalline phases. Let us point out that the migration effect can also lower the elastic moduli.[39]

D. Interaction energy

Interaction energies, like curvature energies, are small in microemulsion systems. They arise from van der Waals forces, screened electrostatic interactions, steric repulsion, . . . Again because the interfacial energies are small, these terms play an important role in determining the phase behavior.

1. *Oil continuous systems*

Interactions have been extensively studied in oil rich systems with light scattering techniques.[44-47] The scattered light intensity is given by:

$$I = I_0 \, \phi \left(\frac{\partial P}{\partial \phi} \right)^{-1} \tag{7}$$

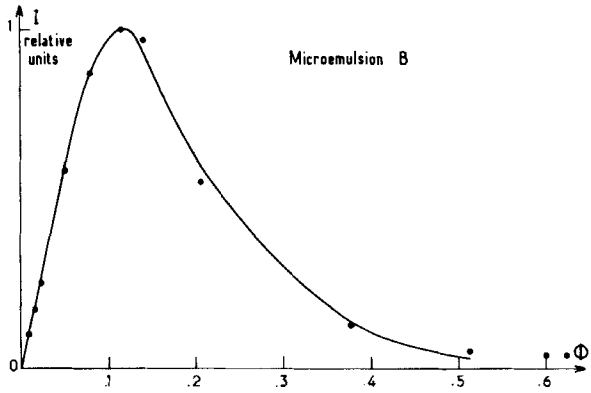

FIGURE 13 Scattered intensity versus droplets volume fraction. The curve is theoretical and the points are experimental; cyclohexane-water-pentanol-SDS microemulsion.

where I_0 is a constant, ϕ the volume fraction of the droplets ($\phi = \phi_w$ in the Talmon-Prager model where the surfactant volume is neglected) and P is the osmotic pressure.

A very convenient description for P when the attraction between droplets is not too large is:

$$P = P_{HS} + \frac{1}{2} A \phi^2 \tag{8}$$

where P_{HS} is the osmotic pressure for a hard spheres system:

$$P_{HS} = \frac{kT}{v_{HS}} \phi_{HS} (1 + \phi_{HS} + \phi_{HS}^2 - \phi_{HS}^3)/(1 - \phi_{HS})^3$$
$$v_{HS} = \frac{4}{3} \pi R_{HS}^3 \tag{9}$$

which is the Carnahan-Starling expression.[48] The hard sphere radius R_{HS} is often smaller than the droplets radius, because two droplets can interpenetrate. The supplementary term $A\phi^2/2$ describe additional interactions as perturbations to the hard sphere potential:

$$A = \frac{4}{kTv} \int_{2R_{HS}}^{\infty} V_A(r) r^2 dr \qquad v = \frac{4}{3} \pi R^3$$

Figure 13 represent the fit of experimental data with the theory; A is equal to -15.5 indicating that attractive forces are present. It has been shown by D. Roux and coworkers that a model of interpenetrating spheres interacting via van der Waals forces lead to theoretical values of A in excellent agreement with the experiments.[47] In this model $R - R_{HS} = l_c - l_{CA}$ where l_{CA} is the cosurfactant chain length.

When A is sufficiently small, phase separation occurs. The critical interaction strength is $A_c = -21$, the critical volume fraction is $\phi_c \simeq 0.13$. This very simple model can thus generate critical points as experimentally observed. It must be recalled that the perturbation expansion of the osmotic pressure Eq. (9) is no longer appropriate to describe the light scattering data close to the critical point.[49] Other attempts using the expressions of Baxter for soft spheres are certainly more appropriate but they do not change very much the critical parameters.[29]

2. Water rich systems

Much less experimental work has been done on the interactions in water rich systems. Electrostatic repulsive forces are expected to be active in ionic surfactant systems. Droplets interpenetration is now unlikely although droplets should have to approach to distances d smaller than the Debye length κ^{-1} to give rise to sufficiently large van der Waals attraction to produce phase separation.[50] Very often, the observed critical points in this domain are lower consolute points, i.e. phase separation occurs, when temperature is raised. It can be shown that conventional interactions like electrostatic and van der Waals forces are unable to give rise to such phase separation when the distance d of minimum approach is fixed: d has to be temperature dependent.[51] The above requirements ($d < \kappa^{-1}$ and temperature dependent) are in contradiction with the finding that for $\kappa R < 1$, the repulsive electrostatic potential is close to a hard sphere potential with $R_{HS} = R + \kappa^{-1}$.[52] The answer to the problem lies may be on the existence of hydration forces[53] like for non-ionic surfactants[54] or on the elongation of the aggregates in order to enhance the van der Waals attraction.

3. Bicontinuous systems

Interactions are probably also effective in these systems. Correlation peaks have been observed in neutron and X-rays scattering experiments which can not be described by the Talmon-Prager theory.[55,56]

They indicate that the oil and water domain have a relatively well defined characteristic size, and that the structure is less random than predicted by the theory. The proper treatment of the interactions between these domains is a still more complicated problem and is far from being solved.

IV. LOW INTERFACIAL TENSIONS

We have seen that microemulsion forms when the oil-water interfacial tension falls below about 10^{-2} dyn/cm. The phase equilibria generated by these systems is very rich and again the interfacial tensions between the coexisting phases are also ultralow. The question then arises, what is the physical origin of these low tensions? Intuitively it may be guessed that in the case of microemulsion formation, the

initial oil-water tension γ_{ow}^0 is lowered by the surfactant via the formation of an interfacial layer having a surface pressure π:

$$\gamma = \gamma_{ow}^0 - \pi \tag{11}$$

In other cases, for instance close to critical points, the tensions are low because the two coexisting phases become similar. The critical scaling theories predict:[57]

$$\gamma = \gamma_0 \epsilon^m \tag{12}$$

where γ_0 is a scale factor, ϵ the distance to the critical point in the phase diagram expressed in terms of a field variable like the chemical potential μ of one component:

$$\epsilon = \frac{|\mu - \mu_c|}{\mu_c}$$

and m is a critical exponent.

Critical points are very frequent in the phase diagrams.[58] This has led several authors[25,59–61] to attribute the low tensions exclusively to critical phenomena, even for the interfaces between oil and water. It can be postulated indeed that as soon as low tensions are evidenced, the interfacial layer has thickened and form a very thin "middle phase" microemulsion.

A. Experimental data

A very careful study of a model system showing the successive Winsor equilibria was undertaken in our laboratory a few years ago[62] and allowed to clarify the problem of the origins of the low tensions. The system was a mixture of toluene (~47 ωt %) water + sodium chloride (~47%), sodium dodecyl sulfate (~2%) and butanol (~4%). The sequence of phase equilibria produced by changing the water salinity S (percentage of NaCl in water by weight) was:

$S < S_1 = 5.4$	Winsor I	O/W microemulsion and excess oil
$S > S_2 = 7.4$	Winsor II	W/O microemulsion and excess water
$S_1 < S < S_2$	Winsor III	middle phase microemulsion, excess oil and water

The interfacial tensions were measured with a very accurate technique, the spectral analysis of the light scattered by the interface.[63] The results are presented on Figure 14. The aspect of the curves is qualitatively the same than for all these type of systems which are models for oil recovery.[64] The tensions are lower in the Winsor III region, and the point where the tension between the microemulsion and the excess oil phase γ_{om} is equal to the tension between the microemulsion and the excess water phase γ_{wm} is called "optimal": $\gamma_{om} = \gamma_{wm} = \gamma^{\star}$. Here $S^{\star} = 6.3$ and $\gamma^{\star} = 4.5\ 10^{-3}$ dyn/cm.

1. Surfactant layers properties

A dilution procedure was found for the microemulsion phases in the WI and WII regions. The interfacial tensions between the excess phases and the continuous phases of the microemulsions are repre-

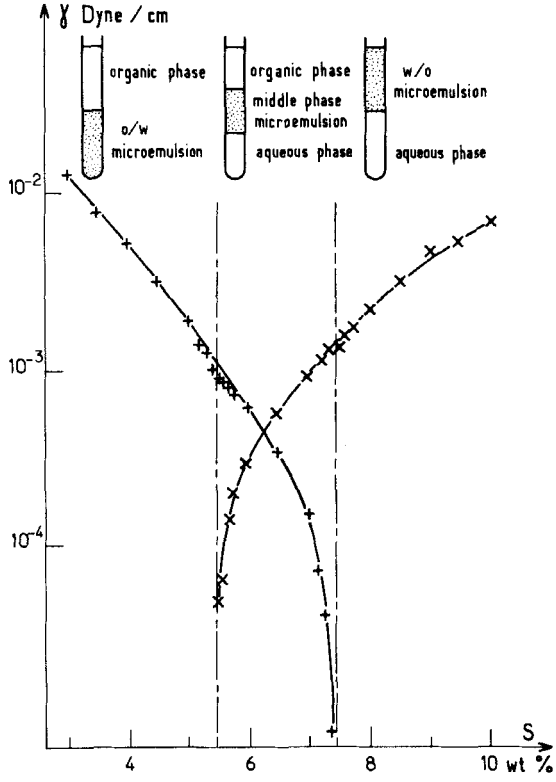

FIGURE 14 Interfacial tensions versus water salinity; + oil-microemulsion interface, × water-microemulsion interface.

sented on Figure 15. In the WIII region the points correspond to the tension between the two excess phases (γ_{ow}). An important remark can be made. These tensions are equal to the largest ones involving the microemulsion phases on Figure 14. The amount of surfactant present in the microemulsion continuous phases or in the excess phases is very small, close to the critical micellar concentration (c.m.c. about 10^{-5} by weight) and no droplets are present: the droplets formation begin above the c.m.c. Like in simple micellar systems, the tensions in the WI and in the WII regions is independent of the droplets concentration. By analogy it can be concluded that the low tension is only due to the high surface pressure of the surfactant layer at the interface.

Although the middle phase microemulsion in the WIII region is not dilutable, the low tensions in Figure 14 are also likely to be due

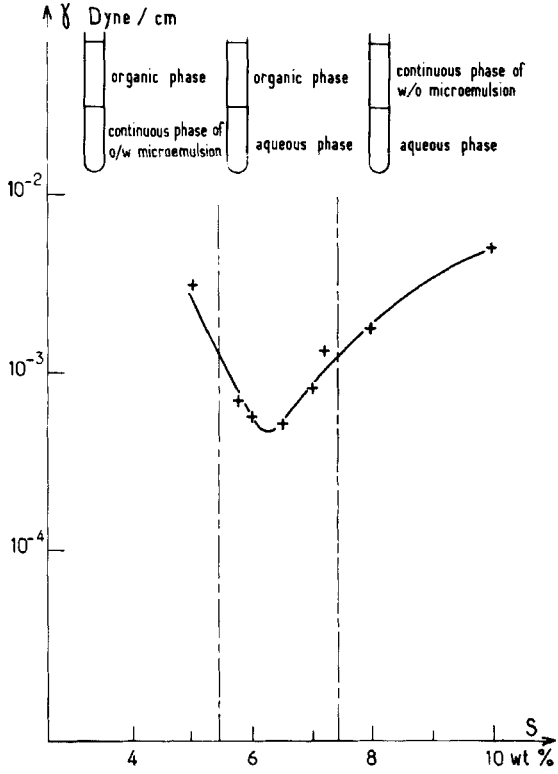

FIGURE 15 Interfacial tensions between excess or continuous phases versus salinity.

to a surfactant layer. The presence of a thin middle phase layer responsible for the low tension can be excluded for the following reasons:

—γ_{ow} is smaller than the sum $\gamma_{mw} + \gamma_{mo}$; if a thin middle phase layer were present, the measured γ_{ow} would be equal to the sum.

—The middle phase does not wet the oil-water interface; this would not be the case if a thin layer of this phase were already present.

2. *Critical behaviour*

The origin of the tensions smaller than $\gamma^{\star}$ was attributed to a different origin. Indeed when the salinity S approaches S_1 the excess water phase becomes turbid before it disappears: the microemulsion turbidity also increases. When S approaches S_2, the excess oil phase behaves in a similar way. This ressembles to critical behaviour, although if S_1 and S_2 where the exact critical points, the interface between the microemulsions and the excess phases would disappear without moving towards the bottom or the top of the sample tube.

Detailed investigation of this critical behaviour has been performed through bulk light scattering experiments, both static and dynamic. Three independent values of the correlation length of the concentration fluctuations ξ_c have been determined close to S_2: from the angular variations of the scattered intensity and of the diffusion coefficient, and from the diffusion coefficient extrapolated at zero scattering angle. The three determinations were in satisfactory agreement. Values of ξ_c up to 800 Å were measured close to S_2. The largest measured ξ_c is only four times the droplet size: this means that S_2 is still relatively far from the true critical point. The other boundary S_1 is still further from the other critical point: bulk light scattering experiments can not be interpreted with the critical phenomena theories even very close to S_1, where the largest measured ξ value is only the droplet size (~200 Å). The data rather indicate that the droplets of the WI region become elongated and polydisperse close to S_1. In these systems we ignored the exact distance to the critical point ϵ since the chemical potentials of the different chemical species were unknown. In order to test the scaling predictions for the interfacial tensions Eq. (12), we used another physical property of the system, experimentally measurable, and showing critical behaviour. The density difference between the two coexisting phases is one of such variable:

$$\Delta\rho = \Delta\rho_0 \epsilon^{\beta} \tag{13}$$

by eliminating ϵ between Eq. (12) and 13, one obtains:

$$\gamma = \gamma_0 \left(\frac{\Delta\rho}{\Delta\rho_0} \right)^{m/\beta} \tag{14}$$

A log log plot of γ versus $\Delta\rho$ is shown on Figure 16. The slope m/β is the same for the two interfaces γ_{om} and γ_{wm}:

$$\frac{m}{\beta} = 4$$

in agreement with the $3d$ Ising exponent. Let us recall that the mean field value of m/β is 3.

From Figure 16 one sees clearly the change in slope above γ^* indicating that critical behavior is no longer followed.

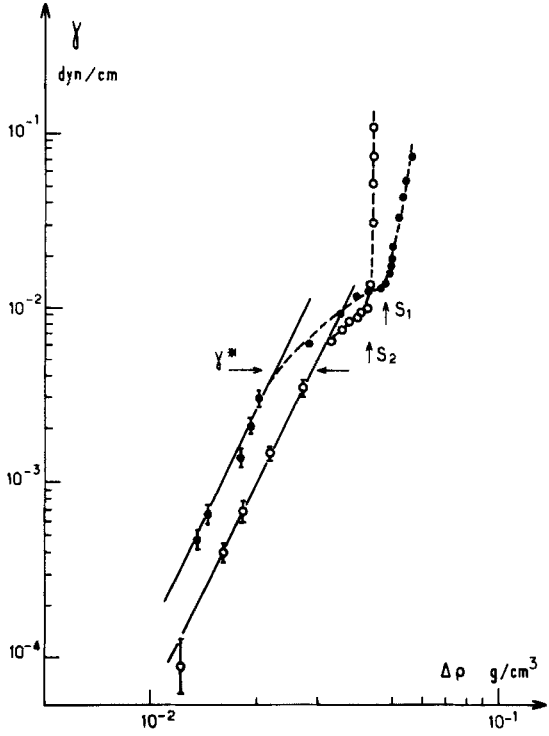

FIGURE 16 Interfacial tensions versus density difference between the coexisting phases; ● water-microemulsion, ○ oil-microemulsion. The lines are theoretical, their slope is 4.

B. Theoretical predictions

1. *Surfactant monolayers*

When a surfactant monolayer is present at the oil-water interface, we have seen that the interfacial tension is lowered by a quantity equal to the surface pressure developed by the monolayer:

$$\gamma = \gamma_{ow}^0 - \pi \tag{15}$$

By introducing the surfactant free energy $G(\Sigma)$, Σ being the area covered by a surfactant molecule, De Gennes has written the total free energy in the form:[34]

$$F = F_{bulk} + \gamma_{ow}^0 A + n_S G(\Sigma) \tag{16}$$

where A is the total interfacial area and n_S the number of surfactant molecules $n_S = A/\Sigma$. F_{bulk} is the bulk free energy and contains the terms discussed in § III if one of the coexisting phases is a microemulsion.

γ and F are related by $\gamma = \partial F/\partial A$; it then follows that:

$$\pi = -\frac{\partial G}{\partial \Sigma} \tag{17}$$

A useful quantity is the surfactant chemical potential:

$$\mu_S = \left.\frac{\partial F}{\partial n_S}\right|_A = G(\Sigma) - \pi(\Sigma)\Sigma \tag{18}$$

this value is equal to the chemical potential of the surfactant in the bulk phases which of course depends on the shape of the aggregates if any, on their concentration and on the interactions between the aggregates. All these properties will then affect the surface tension γ which depends ultimately on μ_S.

2. *Spherical droplets without interactions*

Let us first consider the case where one bulk phase contains spherical droplets without interactions. γ has been derived in this case by J. Israelachvili[65] in the following way: if N is the aggregation number:

$$\mu_S = \mu_N^0 + \frac{kT}{N} \ln \frac{X_N}{N} \tag{19}$$

where μ_N^0 contains the interactions terms between polar and non polar parts of the surfactant in the droplet; X_N is the surfactant concentration present in the droplet (volume fraction).

By using Eqs. (15) to (18) one can show that:

$$\mu_S = \mu_\infty^0 - \gamma\Sigma \tag{20}$$

μ_∞^0 is the limit of μ_N^0 for an infinite aggregation number: flat monolayer.

The interfacial tension is then:

$$\gamma = \frac{1}{\Sigma}\frac{kT}{N}\ln\frac{X_N}{N} + \frac{1}{\Sigma}(\mu_\infty^0 - \mu_N^0) \tag{21}$$

The first term is an entropy contribution γ_E arising from mixing. If the droplets have a radius R then:

$$\gamma_E = -\frac{kT}{4\pi R^2}\ln\frac{X_N}{N} \tag{22}$$

This expression is analogous to the one derived by E. Ruckenstein on different thermodynamical bases.[66]

It could be noted that the order of magnitude of γ_E is kT/R^2, to be compared to the tension between simple liquids which are of the order of kT/a^2, a being a molecular length. This means that if R is 100 times larger than a molecular length, γ_E will be 10^4 times smaller than usual surface tensions.

The second term of Eq. (21) is a curvature contribution γ_C since it includes difference between surfactant interactions in spherical and flat aggregates. This contribution has been explicitly calculated by several authors.[37,67,68] As pointed out recently[32] these calculations are equivalent to:

$$\gamma_C = \frac{K}{2R^2} \tag{23}$$

where K is the curvature modulus. As K is expected to be of the order of kT, γ_C is expected to be of the same order of magnitude than γ_E. As both contributions are inversely proportional to R^2, it will be difficult to distinguish experimentally between the two contributions.

The experimental values of γ in the SDS system are of the same order of magnitude than those calculated from the preceeding theories by using the R experimental values of the WI and WII regions.

It should be noted that γ is inversely proportional to R^2 even at the c.m.c. where the bulk phases contain no droplets. This arises because the chemical potential of the surfactant in the monolayer is equal to the chemical potential of the surfactant in the droplets which depends on R. The properties of the flat monolayer are not independent of the properties of the curved monolayer that it would form if it were not constrained to lye at the flat interface.

3. *Bicontinuous models*

The entropic contribution has been calculated by Talmon and Prager:[69]

$$\gamma_E \sim \frac{kT}{\xi^2} \tag{24}$$

where ξ is the size of the elementary units (the persistence length in the De Gennes model).[32] Again one sees that γ_E is of the order of kT divided by the square of the characteristic size.

Curvature contributions have not been calculated in this case, but they can reasonably be expected to be negligibly small.

ξ measurements were recently performed with X-ray techniques in a dodecane-water-NaCl-butanol-hexadecyl benzene sulfonate (S.H.B.S.) system.[70,71] At the optimal salinity a value of $\xi \sim 386$ Å can be deduced from Guinier Plots, close to the theoretical value of ξ which is:[32]

$$\xi_{th} = \frac{6\phi_o\phi_w}{C_S\Sigma} \tag{25}$$

where ϕ_o and ϕ_w are the oil and the water volume fraction and C_S the number of surfactant molecules per unit volume ($n_S = C_S N\xi^3$ and $\Sigma n_S = 6\phi_o\phi_w N\xi^2$). At the optimal salinity $\phi_o = \phi_w \sim 0.5$ and:

$$\xi_{th}^{\star} = 363 \text{ Å}$$

with $\Sigma = 110$ Å^2, as measured from light and X-rays scattering.[71]

We have performed recently surface tension measurements on this system.[71] At the optimal salinity $\gamma_{exp}^{\star} \sim 8.10^{-4}$ dyn/cm.

ξ measurements are not available for the SDS systems where the experiments deviate seriously from the predictions of the Talmon-Prager model.[55–57] The calculated value at optimal salinity is $\xi^{\star} \sim 220$ Å smaller than in the S.H.B.S. system. The ratio of the two calculated values for the two systems is about 1.6 allowing to predict a ratio of $\gamma^{\star}$ values of about 2.7. The experimental ratio is noticeably larger: 5.6.

It must be noted however that the Talmon-Prager theory applies to an equilibrium between two microemulsions of symmetrical compositions ϕ_w and $1 - \phi_w$. Moreover, the theory predicts an oil rich region close to the oil rich phase (or a water rich region close to the water rich phase). Recent experiments with ellipsometric techniques on various model systems including the SDS one[73,74] indicate rather the opposite situation.

C. Critical behaviour

Interactions have been incorporated in some droplets models within the frame of mean-field treatments.[67,75] They led to tensions that would obviously depend on the droplets volume fraction. This is also true for the entropic term Eq. (21) but as the concentration appears in a logarithm, the variation of tension with the concentration is very small. Let us recall that this was indeed observed in the WI and WII regions far from the WIII region.[62] On the contrary, when the phase boundaries are approached, the interactions between the droplets were observed to increase. Sufficiently close the tensions follow the scaling law:

$$\gamma = \gamma_0 \epsilon^m$$

and the product $\gamma\xi_C^2$ is a universal constant of order kT.[76] Thus again $\gamma \sim kT/\xi_C^2$ form similar to what was found for surfactant layers. This probably explain the smoothness of the surface tension variation when crossing the frontier between the two regimes: surfactant monolayer and critical behaviour. As m is not a mean field exponent, the mean field treatments[67,75] will obviously not be adequate.

In conclusion, the quantitative predictions for surface tension in microemulsions are still incomplete, specially close to critical points. Up to now, the theories are unable to explain the observed features. The interaction forces leading to phase separation in O/W systems remain mostly unknown. These questions will be further discussed in § VII.

On another hand, even far more critical points, the relationship between surface tension and microemulsion structure still deserves more work, specially in the middle phase domain. Some systematic trends have however been tested: γ is about inversely proportional to the square of the characteristic length of the structure (droplets radius or persistence length).

V. PERCOLATION AND INVERSION

A. Droplets structure

The droplet structure was introduced by Schulman and coworkers in order to explain data from light and X-ray scattering, sedimentation, and other techniques. One of the main problems in the interpretation of the experiments is the separation between particles shape and interactions effects. Sometimes it is possible to dilute the system, i.e. to reduce the particles number. For instance by extrapolating the light scattering data to zero particle volume fraction ϕ, one has from Eq. (7) and from the perfect gas limit $P(\phi \to 0) = kT/v\phi$:[77]

$$\lim_{\phi \to 0} \frac{I}{\phi} = I_0 \frac{v}{kT} \qquad v = \frac{4}{3}\pi R^3 \tag{26}$$

The particle radius R is then easily obtained.

1. *Dilution method*

A dilution method for microemulsions was proposed by Schulman[8] and refined later on by A. Graciaa[78] and in our laboratory.[62]

The continuous phase of the droplets has to be determined, and the droplet size has to remain constant when this continuous phase is added to the microemulsion.

The essential hypothesis is to assume that the droplet size in the microemulsions which are in equilibrium with other phases (liquid crystals or excess phases) is constant when the ratio of surfactant to water (or oil) amounts in the droplets is fixed. This is equivalent to assume that the area per surfactant molecule at the droplet surface Σ is independent of the oil (or water) amounts in the continuous phase along the demixing surface (Figure 17).

Then if a W/O microemulsion has to be diluted a certain amount of oil is added in a first step to the microemulsion phase. It usually becomes turbid since the mixture has no longer the composition of a point of the demixing surface (Figure 17). Then alcohol is added

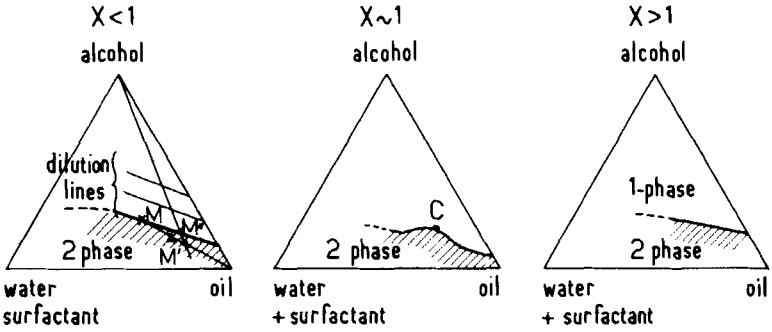

FIGURE 17 Pseudo ternary oil-water-surfactant-alcohol phase diagrams at fixed water/surfactant ratio X. Dilution lines for $X < 1$. Principle of the dilution: $M \rightarrow M'$ in the 2-phase region when oil is added; $M' \rightarrow M''$ in the 1-phase region when alcohol is added. Critical point C around $X \sim 1$. Pseudo dilution line for $X > 1$.

to restore the transparency. This procedure has to be repeated in order to ensure that the ratio of oil and alcohol amounts added are constant. Generally for droplets volume fraction ϕ below a few percent it is necessary to add small water and surfactant amounts in the continuous phase. Similarly the continuous phase of the O/W microemulsions contains water and alcohol and small amounts of oil and surfactant. The surfactant concentrations are about the c.m.c. in the water-alcohol mixtures as it could be expected.

A theoretical calculation based on a pseudophase model where the continuous phase, the interfacial region and the droplets interior are treated like phases in thermodynamical equilibrium allows to describe satisfactorily the existence of dilution lines and to predict their existence even in the single phase domain[79] (Figure 17).

The validity of the dilution procedure has been proved with neutron and light scattering experiments,[80,81,57,28] in several systems where both the droplets volume fraction and the interactions between the droplets were not too large. When interactions become strong, they can lead to changes in shape like in aqueous micellar solutions when they are repulsive and to phase separation when they are attractive. The last case is currently observed in microemulsions and the dilution lines (Figure 17) become strongly curved although droplet size remains constant *along the line* as evidenced from neutron scattering experiments.[28]

The dilution method proper is restricted to the case of straight dilution lines. Its validity is usually limited to small droplets volume fractions $\phi \lesssim 0.1$ and as already said above to weakly interacting droplets.[82] But surprisingly, fairly concentrated "hard sphere" like

systems, up to volume fractions of 0.30–0.40, can also be diluted. These volume fractions are well above the transition towards bicontinuous structures predicted by Talmon and Prager: $\phi_p \sim 0.18$. The explanation of this will be given later on (§ B-1).

2. Droplets aggregates

When interactions between droplets are attractive, the probability of forming aggregates during a collision is significant. The presence of dimers was evidenced at low ϕ (a few percents) in a weakly attractive case with neutron scattering experiments.[83] These dimers were not present in "hard-sphere" systems. Later on, an electrical birefringence study of W/O microemulsions was performed in our laboratory.[84] In this method the aggregates are seen directly because single spheres show no electrical birefringence. The amount of aggregates was observed to increase rapidly with increasing attractive interactions. Giant signals where obtained close to the critical points. This could of course also be related to the closest presence of the liquid crystalline phases (§ II).

B. Percolation

1. Electrical conductivity measurements

The Talmon-Prager model predicts that for $\phi_w \gtrsim 0.18$, the water domains become interspanned. This can be evidenced for instance by a steep increase of the electrical conductivity around ϕ_w. A theoretical treatment of this phenomena has been given by M. Lagües taking into account the transient character of the infinite water domain above ϕ_p.[85] A very successful confirmation of these ideas has been found in W/O microemulsions containing weakly attracting droplets.[86] However we have shown that the variation of electrical conductivity around ϕ_p is steeper when interactions are more attractive and that the "electrical" percolation on the contrary disappears with hard sphere like droplets (Figure 18).[87,84]

Clearly these effects arise because of the presence of the interfacial layer which is neglected in the Talmon-Prager model. When the interfacial layer is rigid, two droplets can not interpenetrate (hard sphere case) and the conductivity of this layer being small, the conductivity of the infinite aggregate of droplets is also small and the percolation can not be evidenced at ϕ_p in this way. When the interfacial layer is more fluid, two droplets can interpenetrate and the resulting van der Waals attraction increases. The mechanisms of conductivity are not still well known: either the water cores become connected during this process,

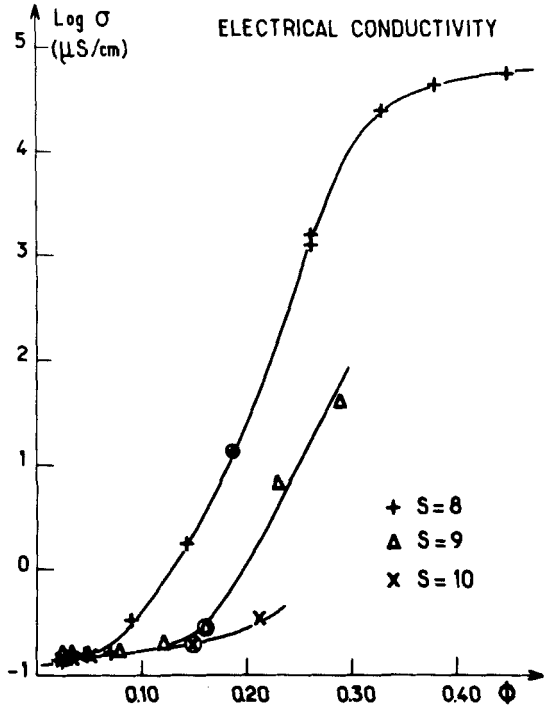

FIGURE 18 Electrical conductivity variation versus droplets volume fraction, for the W/O microemulsions coexisting with excess water (§ IV-a). $S = 10$ corresponds to hard sphere like droplets, $S = 8$ to strongly attractive droplets.

either the conductivity of the interfacial layer becomes high enough to produce the steep increase of the global electrical conductivity.

It must also be noted that the experimental value of ϕ_p decreases with increasingly attractive interactions[84] as expected theoretically, on the basis of interacting sphere models.[88]

In summary the hard sphere systems do not become bicontinuous at ϕ_p. Individual droplets are probably present up to the inversion $\phi \sim 0.50$. This explains why the dilution method is valid up to large ϕ. The weakly attractive systems which can be diluted below ϕ_p, may still contain individual droplets above ϕ_p. This point is far from clear as well as the strongly attractive systems structure is. It may be guessed that the structure progressively evolves towards a bicontinuous structure (Figure 19). Indeed the strongly attractive systems are not dilutable even below ϕ_p as it could be expected from a bicontinuous system.

Let us point out that this discussion is only relevant of W/O systems. The percolation phenomena for the O/W system can not be evidenced with electrical conductivity measurements and the corresponding mechanisms are mostly unknown.

2. Relation to critical behaviour

Critical phenomena and onset of phase separation occurs in strongly attractive systems at a droplets volume fraction ϕ_c. In W/O systems ϕ_c is always close to ϕ_p. This situation is unusual. For instance phase separation can be observed in polymer solutions showing also a sol-gel transition which is another example of percolation phenomena. The polymer gelation concentration is usually very different from its critical concentration.[89] Phase separation in attractive spheres systems has been described with a variety of interaction potential, and of perturbations methods. The striking result is that the critical concentration ϕ_c is always about 0.20,[54] i.e. very close to the percolation thresholds ϕ_p. This coincidence explains why percolation and critical phenomena are observed simultaneously in W/O systems.

Let us recall that the close vicinity of a liquid crystalline phase may also influence the properties of the system. The interpretation of the experiments is therefore extremely complicated. For instance it is not

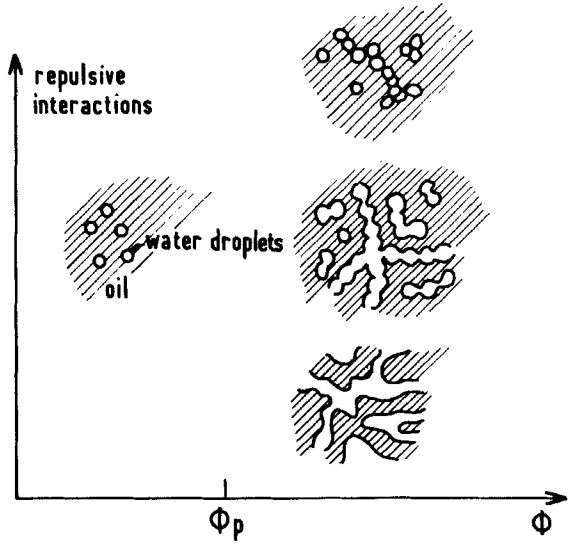

FIGURE 19 Possible structural evolution of W/O microemulsions with increasing droplets volume fraction for hard sphere like and attractive droplets.

clear whether the strong increase in electrical birefringence (§ A-2) is due to critical behavior or to the close presence of a lamellar phase.

A still completely open problem is the nature of interactions above the critical point. Dilution is no longer possible and the existing X-ray or neutron structural studies remains scarce.[56,57] Although theory predicts that above the critical point two phases are obtained, a droplets rich phase ($\phi_1 > \phi_c$) and a droplets poor phase ($\phi_2 \ll \phi_c$, due to the assymmetry of the coexistence curve), single phase microemulsions of intermediate concentration can still be obtained for instance by adding a little more alcohol to the mixture. The structure and the interactions in these systems are completely unknown despite of the fact that they are extremely frequently encountered. Let us take for instance the case of oil rich systems. Attraction between droplets increases with the volume of interpenetration of two droplets, which is for a given surfactant-cosurfactant interfacial layer, a increasing function of the droplet size.[47] As Σ is fixed, this size depends on the water to surfactant ratio X (by weight). Experimentally the critical points are frequently found around $X = 1$. All the single phase mixtures for which $X \gtrsim 1$ will be over-critical (Figure 17).

C. The inversion domain

In the Talmon-Prager model, the inversion from W/O towards O/W structures is very progressive and is encountered for water volume fractions ϕ_w between about 0.18 and 0.82. The experiments show that the model does not apply to all the microemulsion systems. In the hard-sphere systems the inversion is certainly much sharper. Electrical birefringence data show the existence of large and fast interfacial orientation fluctuations around $\phi_w \sim \phi_o$: they could correspond to curvature inversion.[84] When the interaction between the droplets increases, these fluctuations remains and are still only present in a sharp volume fraction range. This may indicate that droplets are still present above ϕ_p and that percolation and inversion are independent processes.

Very little is known about the over-critical systems. The electrical conductivity varies linearly with water volume fraction as expected from effective medium theories.[84,90,91] This is not observed even above ϕ_p for the sub-critical systems.[84,86,87] This might indicate that the over-critical systems are truly bicontinuous and that the inversion domain is extended, between ϕ_p and $1 - \phi_p$.

VI. DYNAMIC PROPERTIES

Microemulsion structures are transient. The renewal times τ are extremely short, in the microsecond range or shorter. A quantitative difference is found between systems with or without cosurfactant. Cosurfactant molecules are small molecules and favour rapid exchanges. For this reason microemulsions containing cosurfactant are even sometimes considered as molecular mixtures. A clear distinction has to be done on several bases:

—static measurements like scattering of electromagnetic radiation give an instantaneous picture of the medium. For instance, if well defined interfaces are present, X-ray or neutron scattering data will follow the Porods' law:[92]

$$\lim_{q \to \infty} q^4 I(q) = cte ,$$

q being the scattering wave vector, I the scattered intensity;

—dynamic measurements with a characteristic time τ_m will reveal structural features only if $\tau_m \ll \tau$. In the case $\tau_m \gg \tau$ average properties will be measured. For instance quasielastic light scattering operates in the range $\tau_m \gtrsim 10$ μs. For diluted microemulsions, it indicates the presence of droplets of small polydispersity when no cosurfactant is used. The polydispersity usually disappears when alcohol is present. Quasielastic neutron scattering with spin echo methods, which operates in the 10 ns range, indicates on the contrary an enormous polydispersity in the same systems.[93]

A. Molecular exchanges

Ultrasonic relaxation studies of a large variety of diluted or concentrated microemulsions, have revealed the existence of two relaxation processes in the Megahertz range when alcohol is present.[94] These two processes were associated to the exchanges of the surfactant and of the alcohol between the interfacial film and the oil or water domains. The characteristic time for the exchange of the alcohol is always at least ten times shorter than that for the surfactant.

Chemical relaxation methods have shown that the response of these systems to perturbations involve two kinds of characteristic times: fast processes associated to surfactant exchanges like in ultrasonic relaxation and a slow process associated to the interfacial film formation and breakdown, as a whole. A systematic study of the effect

of oil addition to mixed alcohol surfactant aqueous micelles showed that the formation of microemulsions is accompanied by a rapid increase of the characteristic time τ_s of the slow process: τ_s increases by factors up to 10^4 and reaches values of the order of seconds.[95] The interfacial films in microemulsions seem therefore only renewed by exchanges of single surfactant molecules.

The transport of matter between oil and water regions has been investigated through chemical reactivity and fluorescence decay studies.

In water in oil microemulsions the transport of matter occur through collisions and transient merging of water droplets. B. Robinson and coworkers measured by stopped flow techniques the rate of chemical reactions involving transfer of water contents. In AOT-heptane-water systems they showed that about one collision per thousand is effective.[96] In microemulsions containing alcohol the exchange rate becomes too fast to be measured in this way.[97] Atik and Thomas investigated this exchange rate with fluorescence decay studies. They showed that the nature of the alcohol strongly influence the exchange rate.[98] The increase in exchange rate reveals the increase of the interfacial layer fluidity. As pointed out in § V-B, droplets fusion is favoured with fluid layers.

In oil in water microemulsions the exchange processes are still less known. They cannot occur through collisions owing to the electrostatic repulsion between droplets. They probably involve a partial breakdown, or a fragmentation.[13]

B. Transport properties

The transport of electric charges occurs on a time scale much shorter than the microemulsion structure lifetimes. The electrical conductivity is therefore a probe of the water connectivity of the structure (§ V-B).

On the opposite, viscosity measurements are made on a time scale much longer than all the renewal times. Viscosity reflects therefore an average behaviour of the systems. Viscosity maxima are currently observed around the percolation transitions: ϕ_o or $\phi_w \simeq 0.2$.[91] They are not yet satisfactorily interpreted.

Sedimentation and quasielastic light scattering have frequently been used to measure the droplets hydrodynamic radius R_H in diluted microemulsions. The friction coefficient f_{sed}, as measured in a sedi-

mentation experiment and the mutual diffusion coefficient D_m as measured by QELS are:[46]

$$f_{sed} = 6\pi\eta_0 R_H(1 + \beta\phi) \tag{27}$$

$$D_m = \frac{\partial P/\partial\phi}{f_m} = \frac{kT}{6\pi\eta_0 R_H}(1 + \alpha\phi) \tag{28}$$

where η_0 is the viscosity of the continuous phase, ϕ the droplets volume fraction, P the osmotic pressure and f_m a friction coefficient related to f_{sed} by:

$$f_{sed} = f_m(1 - \phi) \tag{29}$$

The extrapolation of f_{sed} and D_m to zero droplets volume fraction leads generally to the same hydrodynamic radius, close to the effective radius R of the droplet as deduced from static scattering experiments: $R_H = R$ for hard sphere droplets, $R_H > R$ for soft or elongated droplets. But the concentration variations of f_{sed} and D_m cannot be predicted by the hydrodynamic theories for permanent particles (Figure 20). Clearly the exchanges play a role in this concentration variation.[45,46]

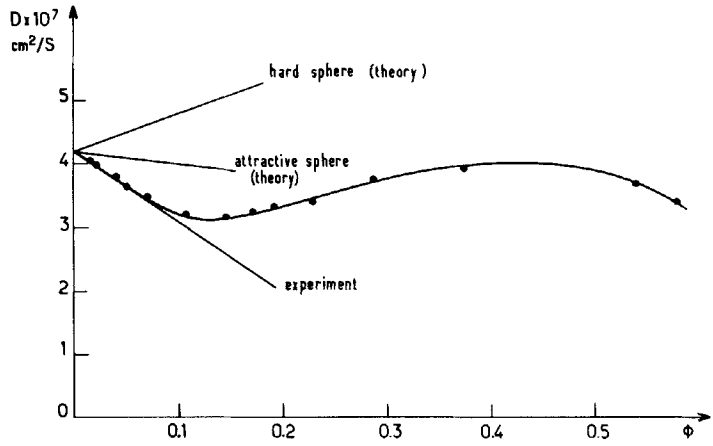

FIGURE 20 Diffusion coefficient versus droplets volume fraction. The points are experimental. Theoretical lines at small volume fraction are given for comparison. Cyclohexane-water-SDS-pentanol microemulsion.

It has to be pointed out that the D_m versus ϕ variation is frequently significant. The hydrodynamic radius can not therefore be calculated directly from D_m by setting $\alpha \approx 0$ and using the Stoke-Einstein relation. A dilution, and an extrapolation to $\phi = 0$ has to be performed.

In the bicontinuous microemulsions, there exists only theoretical predictions for D_m by Kaler and Prager in the range $q\xi \gtrsim 1$ where q is the scattering wave vector.[99] Unfortunately the experiments correspond frequently to $q\xi \ll 1$. It can be noted however that D_m is usually about 10 times lower than the equivalent Stokes-Einstein coefficient $D_m^{\star} = kT/6\pi\eta\xi$, η being the microemulsion viscosity. This might reflect again the role of the exchanges.

Tracer diffusion coefficients D_t appear to be more related to the microstructure. For instance if the characteristic time of the measurements is shorter than the renewal times, D_t reflects the connectivity of the structure like the electrical conductivity reflects the water connectivity. For instance if the tracer is solubilized in the droplets. D_t is equal to the droplet self diffusion coefficient D_{self} and if the tracer is solubilized in a continuous phase D_t is approximately equal to its value in the pure phase: D_{free}. For diluted droplets:

$$D_{\text{self}} = \frac{kT}{6\pi\eta_0 R_H}(1 + \alpha'\phi) \tag{30}$$

α' and α are usually of opposite signs for repulsive droplets.[100]

There exists a variety of experimental techniques allowing to measure D_t in microemulsions: radioactive tracers,[101] spin echo NMR,[102] forced Rayleigh scattering,[100] photobleaching recovery.[103] In diluted microemulsions, the diffusion coefficient of tracers solubilized in the droplets are in fairly good agreement with Eq. (30). When the percolation threshold is approached in water in oil microemulsions a striking phenomenon occurs: for the tracers solubilized in the interfacial films D_t as measured from radiotracers and NMR increases, whereas D_t as measured from forced Rayleigh and photobleaching methods decreases (Figure 21). Theory predicts that D_t should go to zero: connectivity fluctuations diverge at a percolation point in the same manner that concentrations fluctuations diverge at a critical point ($D_m \rightarrow 0$).[104] Here D_t decreases only by factors of order unity (when it decreases). Clearly the motion of the tracer along the infinite aggregate formed at the percolation threshold is perturbed by the breakdown of this aggregate. D_t might even increase if the tracer is exchanged rapidly between the film and the water and oil domains (as observed in NMR).

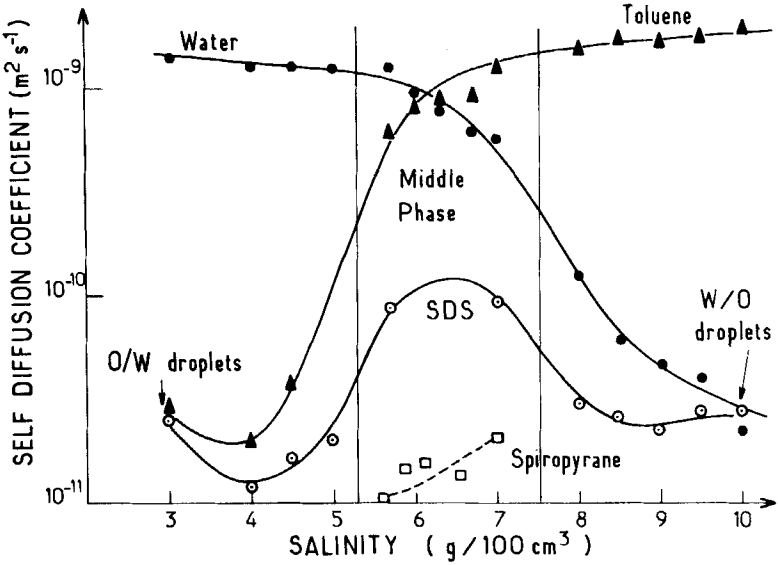

FIGURE 21 Self diffusion coefficient of different species in the microemulsion of § IV-a versus salinity: toluene, water and SDS from NMR and spyropyran from forced Rayleigh experiments.

The interpretation of the tracer diffusion coefficients in microemulsions is therefore very difficult. A better knowledge of the exchange processes is certainly needed to interpret the data in the concentrated systems.

In conclusion, the dynamic behavior of microemulsions is very rich. It remains poorly understood, in many aspects, specially for the microemulsions containing comparable amounts of oil and water. Its role is however fundamental in some important applications like chemical reactivity. This dynamic behaviour is probably the microemulsions property that distinguish them the most from liquid crystalline phases. The fast molecular exchanges make them closer to molecular mixtures.

VII. CONCLUSION

Microemulsions contain oil and water microdomains separated by surfactant layers like lyotropic liquid crystals. The flexibility of the surfactant layers are much larger in microemulsions. For this reason they form structures much less organized, either small droplets or distorted lamellar phases. Amongst them, different degrees of layer

flexibility can be encountered: the more rigid corresponds to a system without cosurfactant or with a long chain one; the more fluid correspond to short chain cosurfactants. A great variety of behaviour are associated to these different systems: the more rigid lead to hard sphere-like droplets, the more fluid to bicontinuous-like structures.

The study of the defects of the liquid crystalline structures nearby the microemulsions in the phase diagram is promising. As in simpler water-surfactant-alcohol mixtures, these defects might prefigurate the microemulsion structure.

The presence of the surfactant layers and their high flexibility are fundamental in reaching ultralow interfacial tensions in microemulsion systems. Still lower tensions are obtained close to the critical points which are extremely frequent in the phase diagrams. The study of these critical points deserve further work. It is not clear whether the order parameter for critical behavior is as simple as in molecular mixtures or if it is more complex like in the transitions between liquid crystalline phases.

The dynamic properties of the microemulsions are largely determined by the molecular exchanges between the surfactant layers and the water and the oil microdomains. These exchanges are much more important than in the lyotropic liquid crystalline phases. For chemical reactivity purposes for instance, microemulsions with very flexible layers behave more like molecular mixtures.

The great variety of structure and of behavior make microemulsions very attractive systems for fundamental research as well as for applications.

References

1. "*Microemulsions*," Ed. L. M. Prince, Acad. Press, 1977.
2. I. Rico and A. Lattes, *J. Coll. Int. Sci.*, **102**, 285 (1984); S. Friberg, "Non aqueous micromulsions" CRC Press, 1986.
3. P. Ekwall, "*Advances in Liquid Crystals*," **1**, 1 (1975).
4. M. Dvolaitzky, R. Ober, J. Billard, C. Taupin, J. Charvolin and Y. Hendriks, *C. R. Hebd. Sean. Acad. Sci.* B, **295**, 45 (1981).
5. I. Danielsson and B. Lindman, *Colloids Surf.*, **3**, 391 (1981).
6. H. F. Eicke and P. Kvita, in "*Reverse Micelles*," Ed. P. L. Luisi and B. E. Straub, Plenum Press, 1984.
7. T. P. Hoar and J. H. Schulman, *Nature* (London) **152**, 102 (1943).
8. J. H. Schulman, W. Stoeckenius and L. M. Prince, *J. Phys. Chem.*, **63**, 1677 (1959).
9. E. Ruckenstein and J. Chi, *J. Chem. Soc., Faraday Trans.* 2, **71**, 1690 (1975).
10. "*Surface Phenomena in Enhanced Oil Recovery*," Ed. D. O. Shah, Plenum Press, 1981.
11. S. Friberg, *J. Coll. Int. Sci.*, **56**, 19 (1976).

12. L. E. Scriven, in "*Micellization, Solubilization and Microemulsions*," Ed. K. L. Mittal, Plenum, 1977.
13. Z. Zana, in "*Surfactants in Solution*," Ed. K. L. Mittal and P. Bothorel, Plenum, 1986.
14. J. H. Fendler and E. J. Fendler, "*Catalysis in Micellar and Macromolecular Systems*," Ac. Press, N.Y. (1975).
15. F. Candau, U. S. Leong, G. Pouyet and S. Candau, *J. Coll. Int. Sci.*, **101**, 167 (1984).
16. J. H. Fendler, in "*Reverse Micelles*," Ed. P. L. Luisi, Plenum (1982).
17. J. Kiwi and M. Graetzel, *J. Phys. Chem.*, **84**, 1503 (1980).
18. P. Speiser, in "*Reverse Micelles*," Ed. P. L. Luisi, Plenum (1982).
19. B. Clin, M. Barthe, J. Biais, M. Bourrel and P. Lalanne, in "*Surfactants in Solutions*," Ed. P. Bothorel and K. L. Mittal, Plenum (1986).
20. Y. Hendriks and J. Charvolin, *J. Phys.*, **42**, 1427 (1981).
21. P. A. Winsor, "*Solvent Properties of Amphiphilic Compounds*," Butterworths' Scientific publication, London (1954).
22. R. N. Healy, R. L. Reed and D. G. Stenmark, *Soc. Pet. Eng. J.*, 147 (June 1976).
23. A. M. Bellocq, J. Biais, B. Clin, A. Gelot, P. Lalanne and B. Lemanceau, *J. Coll. Int. Sci.*, **74**, 311 (1980).
24. H. Kunieda and K. Shinoda, ref. 1, chap. 4 and *J. Coll. Int. Sci.*, **75**, 601 (1980).
25. M. Kahlweit, *J. Coll. Int. Sci.*, **90**, 197 (1982); M. Kahlweit, E. Lessner and R. Strey, *J. Phys. Chem.*, **87**, 5032 (1983).
26. J. C. Lang and B. Widom, *Physica A (Amsterdam)* **81A**, 190 (1975).
27. S. Friberg, in ref. 1.
28. D. Roux, Thesis Bordeaux 1984.
29. D. Roux, A. M. Bellocq and M. S. Leblanc, *Chem. Phys. Lett.*, **94**, 156 (1983).
30. A. Zrabda, 3e cycle Thesis, Pau, 1984. M. Clausse, A. Zrabda and L. Nicolas-Morgantini, *C. R. Acad Sci. Paris*, **296**, 237 (1983).
31. S. J. Chen, D. Fennel Evans and B. W. Ninham, *J. Phys. Chem.*, **88**, 1631 (1984).
32. J. M. Di Miglio, M. Dvolaitzky, R. Ober and C. Taupin, *J. Phys. Lett.*, **44**, L-229 (1983).
33. Y. Talmon and S. Prager, *J. Chem. Phys.*, **69**, 2984 (1978).
34. P. G. De Gennes and C. Taupin, *J. Phys. Chem.*, **86**, 2294 (1982).
35. W. D. Bancroft and C. W. Tucker, *J. Phys. Chem.*, **31**, 1680 (1927).
36. D. J. Mitchell and B. W. Ninham, *J. Chem. Soc. Faraday Trans.* 2, **77**, 601 (1981).
37. M. L. Robbins, in "*Micellization, Solubilization and Microemulsions*," Vol. 2, Ed. K. L. Mittal, Plenum, New York, 1977, p. 273.
38. R. Cantor, *Macromolecules*, **14**, 1186 (1981).
39. W. Helfrich, *Z. Naturforsch.* C, **28**, 693 (1973).
40. S. A. Safran and L. A. Turkevich, *Phys. Rev. Lett.*, **50**, 1930 (1983).
41. B. Widom, *J. Chem. Phys.*, **81**, 1030 (1984).
42. P. G. De Gennes, "*The Physics of Liquid Crystals*," Oxford Press, 1974, p. 111.
43. S. A. Safran, L. A. Turkevich and P. Pincus, *J. Phys. Lett.*, **45**, L69 (1984).
44. A. J. Caljé, W. G. M. Agterof and A. Vrij, in "*Micellization, Solubilization and Microemulsions*," Ed. K. L. Mittal, Plenum Press (1977), p. 779.
45. W. M. Brouwer, E. A. Nieuwenhuis and M. Kops-Verkhoven, *J. Coll. Int. Sci.*, **92**, 57 (1983).
46. A. M. Cazabat and D. Langevin, *J. Chem. Phys.*, **74**, 3148 (1981).
47. B. Lemaire, D. Roux and P. Bothorel, **87**, 1023 (1983); D. Roux, A. M. Bellocq and P. Bothorel, in "*Surfactants in Solutions*," Ed. B. Lindman and K. L. Mittal, Plenum Press (1984).
48. N. F. Carnahan and K. E. Starling, *J. Chem. Phys.*, **51**, 635 (1969).
49. A. M. Cazabat and D. Langevin, unpublished data.

50. V. A. Parsegian, in "*Physical Chemistry: Enriching Topics from Colloid and Surface Science*," Ed. H. Van Olphen and K. Mysels, Theorex, La Jolla, (1975).
51. L. Reatto and M. Tau, *Chem. Phys. Lett.*, **108**, 292 (1984).
52. D. Bendedouch, PhD Thesis, MIT (1983).
53. B. W. Ninham, *J. Phys. Chem.*, **84**, 1423 (1980).
54. R. Kjellander, *J. Chem. Soc. Faraday Trans.* 2, **78**, 2025 (1982).
55. L. Auvray, J. P. Cotton, R. Ober and C. Taupin, *J. Phys.*, **45**, 913 (1984).
56. A. De Geyer and J. Tabony, *Chem. Phys. Lett.*, *Chem. Phys. Lett.*, **113**, 83 (1985).
57. B. Widom, in "*Fundamental Problems in Statistical Mechanics*," Vol. 3, Ed. E. D. G. Cohen, North Holland (1975).
58. A. M. Bellocq, D. Bourbon, B. Lemanceau and G. Fourche, *J. Coll. Int. Sci.*, **89**, 427 (1982).
59. H. T. Davis and L. E. Scriven, *Soc. Pet. Eng. J.*, paper 9278 (1980).
60. P. D. Fleming, III, J. E. Vinatieri, G. R. Glinsmann, *J. Phys. Chem.*, **84**, 1526 (1980).
61. M. W. Kim, J. S. Huang and J. Bok, SPE paper 10788, 911 (1982).
62. A. M. Cazabat, D. Langevin, J. Meunier and A. Pouchelon, *Adv. Coll. Int. Sci.*, **16**, 175 (1982); A. Pouchelon, D. Chatenay, J. Meunier and D. Langevin, *J. Coll. Int. Sci.*, **82**, 418 (1981).
63. D. Langevin, J. Meunier, D. Chatenay, in "*Surfactants in Solution*," Ed. B. Lindman and K. L. Mittal, Plenum Press (1984).
64. W. H. Wade, J. C. Morgan, R. S. Schechter, J. K. Jacobson and J. L. Salager, *Soc. Pet. Eng. J.*, paper 6844 (1977).
65. J. Israelachvili, in "*Surfactants in Solution*," Ed. P. Bothorel and K. L. Mittal, Plenum Press, 1986.
66. E. Ruckenstein, in "*Surfactants in Solution*," Ed. B. Lindman and K. L. Mittal, Plenum Press, (1984) and *Soc. Pet. Eng. J.*, 583 (October 1981).
67. C. Huh, *Soc. Pet. Eng. J.*, paper 10728 (1982) and *J. Coll. Int. Sci.*, **97**, 201, (1984).
68. D. J. Mitchell and B. W. Ninham, *J. Phys. Chem.*, **87**, 2996 (1983).
69. Y. Talmon and S. Prager, *J. Chem. Phys.*, **76**, 1535 (1982).
70. E. W. Kaler, H. T. Davis and L. E. Scriven, *J. Chem. Phys.*, **79**, 5685 (1983).
71. D. Guest, L. Auvray and D. Langevin, *J. Phys. Lett.*, **46**, L-1055 (1985).
72. O. Abillon, D. Chatenay, D. Guest, D. Langevin and J. Meunier, "*Surfactants in Solution*," Ed. P. Bothorel and K. L. Mittal, Plenum Press, 1986.
73. D. Beaglehole, M. T. Clarkson and A. Upton, *J. Coll. Int. Sci.*, **101**, 330 (1984).
74. L. Tenebre, G. Haouche and B. Brun, in "*Surfactants in Solution*," Ed. P. Bothorel and K. L. Mittal, Plenum Press, 1986.
75. C. A. Miller, R. Hwan, W. H. Benton and T. Fort, *J. Coll. Int. Sci.*, **61**, 554 (1977).
76. E. Brezin and S. Feng, *Phys. Rev.* B, **29**, 472 (1984).
77. C. Tanford, "*Physical Chemistry of Macromolecules*," Wiley (1961) p. 217.
78. A. Graciaa, Thesis, Pau (1978).
79. J. Biais, P. Bothorel, B. Clin and P. Lalanne, *J. Disp. Sci. Tech.*, **2**, 67 (1981).
80. M. Dvolaitzky, M. Guyot, M. Lagües, J. P. Le Pesant, R. Ober, C. Taupin and C. Sauteray, *J. Chem. Phys.*, **69**, 3279 (1978).
81. A. M. Cazabat, D. Langevin and A. Pouchelon, *J. Coll. Int. Sci.*, **73**, 1 (1980).
82. A. M. Cazabat, *J. Phys. Lett.*, **44**, L-593 (1983).
83. R. Ober and C. Taupin, *J. Phys. Chem.*, **84**, 2418 (1980).
84. A. M. Cazabat, D. Chatenay, D. Langevin and J. Meunier, *Faraday Discuss. Chem. Soc.*, **76**, 291 (1982).
85. M. Lagües, *J. Phys. Lett.*, **40**, L-331 (1979).
86. M. Lagües, R. Ober and C. Taupin, *J. Phys. Lett.*, **39**, L-487 (1978).
87. A. M. Cazabat, D. Chatenay, D. Langevin and A. Pouchelon, *J. Phys. Lett.*, **41**, L-441 (1980).

88. Y. C. Chiew and E. D. Glandt, *J. Phys. A*, **16**, 2599 (1983).
89. A. Coniglio, E. Stanley and W. Klein, *Phys. Rev. Lett.*, **42**, 518 (1979).
90. J. Peyrelasse, C. Boned, J. Heil and M. Clausse, *J. Phys. C*, **15**, 7099 (1982).
91. K. E. Bennett, J. C. Hatfield, H. T. Davis, C. W. Macosko and L. E. Scriven, in "*Microemulsions*," Ed. I. D. Robb, Plenum (1982).
92. G. Porod, *Koll. Z.*, **124**, 83 (1951).
93. P. Pusey, in *Proc. S.I.F.*, Course XC, Ed. V. Degiorgio and M. Corti, Amsterdam (1985).
94. J. Lang, A. Djavanbakht and R. Zana, in "*Microemulsions*," I. D. Robb Ed. Plenum (1982).
95. J. Lang, in "*Surfactants in Solution*," Ed. K. L. Mittal, P. Bothorel, Plenum (1985).
96. P. Fletcher and B. H. Robinson, *Ber. Bunsenges. Phys. Chem.*, **85**, 863 (1981).
97. B. H. Robinson, private communication.
98. S. Atik and J. Thomas, *J. Phys. Chem.*, **85**, 3921 (1981).
99. E. W. Kaler and S. Prager, *J. Coll. Int. Sci.*, **86**, 359 (1982).
100. A. M. Cazabat, D. Chatenay, D. Langevin, J. Meunier and L. Leger, in "*Surfactants in Solution*," Ed. K. L. Mittal and B. Lindman, Plenum (1984).
101. F. Larche, J. Rouviere, P. Delord, B. Brun and J. L. Dussossoy, *J. Phys. Lett.*, **41**, L-437 (1980).
102. P. Guering and B. Lindman, Langmuir, **1**, 464 (1985).
103. D. Chatenay, P. Guering, W. Urbach, A. M. Cazabat, D. Langevin, J. Meunier, L. Leger and B. Lindman, in "*Surfactants in Solution*," Ed. P. Bothorel and K. L. Mittal, Plenum (1986); D. Chatenay, W. Urbach, A. M. Cazabat and D. Langevin, *Phys. Rev. Lett.*, **54**, 2253 (1985).
104. P. G. De Gennes, *J. Phys. Lett.*, **40**, 199 (1979).